PHYSICAL REVIEW C **89**, 062801(R) (2014)

Shell-model studies of the astrophysical rapid-proton-capture reaction ^{30}P(p,γ)^{31}S

B. Alex Brown,[1] W. A. Richter,[2,3] and C. Wrede[1]

[1]*Department of Physics and Astronomy and National Superconducting Cyclotron Laboratory, Michigan State University, East Lansing, Michigan 48824-1321, USA*

[2]*iThemba LABS, P.O. Box 722, Somerset West 7129, South Africa*

[3]*Department of Physics, University of the Western Cape, Private Bag X17, Bellville 7535, South Africa*

(Received 23 February 2014; revised manuscript received 28 April 2014; published 30 June 2014)

The thermonuclear rate of the reaction ^{30}P(p,γ)^{31}S is important for interpreting nova nucleosynthesis in the $A \geqslant 30$ region. Estimates based on shell-model calculations are complicated by high level density and the presence of negative-parity states in the resonance region near the proton-emission threshold. We present results for the first time of calculations in a full $1\hbar\omega$ model space for the negative-parity states. Spectroscopic factors and proton-decay widths are calculated for input into the reaction rate. Available experimental data are used in conjunction with the calculations to obtain an estimate for the reaction rate. We show that the reaction rate will be uncertain to within about an order of magnitude until the position and decay widths of several of the key states in the region of 6.0 to 6.6 MeV are experimentally determined.

DOI: 10.1103/PhysRevC.89.062801 PACS number(s): 26.30.−k, 21.60.Cs, 21.10.Sf, 21.10.Tg

In nova outbursts on oxygen-neon (ONe) white dwarfs, the ^{30}P(p,γ)^{31}S reaction plays a crucial role in the synthesis of heavier nuclear species, from Si to Ca [1–4]. A classical nova is a thermonuclear explosion on the surface of a white dwarf star accreting hydrogen-rich gas from a companion star in a binary system. In such explosive stellar environments, which include classical novae and x-ray bursters, thermonuclear radiative capture reactions on unstable nuclei determine the path of nucleosynthesis toward the proton drip line. These processes are often dominated by resonant capture to excited states above the particle-emission threshold and therefore depend critically on the nuclear properties of the levels involved. Models have shown that the ^{30}P(p,γ)^{31}S reaction is a potential bottleneck for nucleosynthesis toward heavier nuclei, partly because of the long β-decay half-life ($T_{1/2} = 2.5$ min) of ^{30}P, which is comparable to the duration of nova nucleosynthesis. Its reaction rate, however, is not well determined due to uncertainties in the properties of key resonances in the burning region. This lack of knowledge of the thermonuclear reaction rate inhibits the interpretation of observables associated with the underlying astrophysics. The uncertainties in the reaction rate stem from unmeasured quantities, ambiguities in level properties measured in different experiments, and problems with theoretical calculations stemming mainly from the presence of several negative-parity states near the threshold energy [5–19]. The uncertain ^{30}P(p,γ)^{31}S rate also affects constraints on nova nucleosynthesis via potential nova thermometers recently proposed [20].

The theory for positive-parity states is based on the USDB-cdpn Hamiltonian as used in our previous (p,γ) rate calculations for positive-parity final states in the *sd* shell [21–23]. In a recent paper [24], experimental data were compared with USDB-cdpn results to obtain suggested matches for 29 states below 6.7 MeV in ^{31}S. At the high excitation energies considered here, many negative-parity states start to appear. This paper considers for the first time a microscopic model for these states. The basis consists of a complete $1\hbar\omega$ basis made from all possible excitations of one nucleon from $0p$ to $1s$-$0d$ or the excitation of one nucleon from $1s$-$0d$ to $0p$-$1f$. The *M*-scheme dimension in this basis is on the order of 2×10^6 and they are calculated with NuShellX in a proton-neutron basis [25]. We use the WBP Hamiltonian from [26] that was designed to reproduce the energies of $1\hbar\omega$ states for $A = 10$–20. WBP also contains the sd-pf Hamiltonian from [27] that was designed to reproduce energies of $1\hbar\omega$ states in nuclei with $A = 35$–43. WBP has not before been applied to the middle of the *sd* shell due to the large dimensions involved.

The experimental and theoretical results are shown in Table I and Fig. 1. Columns 2–7 give the experimental data. The spin-parity is given in format $2J\pi$. Columns 3 and 4 are the values given in the recent Nuclear Data Sheets (NDS) compilation [5], and the second column is the resonance energy based on the NDS energy. The fifth column gives the spin-parity assignments from the recent review by Wrede [28] that are based purely on the data for ^{31}S, which excludes spin-parity assignments based upon assumed correspondence with mirror levels in ^{31}P. The spin-parity values for the other references included inside the [ ] brackets in columns 6 and 7 are from assumed mirror assignments and are sometimes adopted from previous work. The letters (a,b,c) in column 5 correspond to the footnotes given by Wrede. For (a) there is some question of whether there are two or three levels between $E_x = 6390$ and 6405 keV. If one assumes that the two levels seen in Ref. [8] are at their reported energies, then one of the two levels reported in Refs. [9,12] and [7] is different and there would be three levels all together. For (b) there are conflicting spin-parity assignments between Parikh *et al.* [9] and Doherty *et al.* [8]. The spin-parity of the 6139 keV state by Doherty *et al.* [8] is based only on a possible match to a level in ^{31}P, but Irvine *et al.* [7] suggested an alternative match. For (c) the spin-parity is unconstrained. The * indicates levels of questionable existence. The levels at 5959 and 6848 keV that are only seen in a low resolution (p,d) experiment [14] are probably amalgams of neighboring levels. The level at 6421 keV has only been seen in a ^{31}Cl β-decay experiment [29] and not confirmed in a reaction experiment. The level

TABLE I. Properties of levels in ^{31}S between 5.9 and 7 MeV. See text for details.

n	Experiment						Theory					
	E_{res} (keV)	E_x (keV)	$(2J)\pi$				USDB-cdpn			$1\hbar\omega$			
							$(2J)\pi$	k	E_x (keV)	$(2J)\pi$	k	E_x (keV)	
		NDS 2013 [5]	NDS 2013 [5]	Wrede 2014 [28]	Doherty *et al.* 2012 [8]	Parikh *et al.* 2011 [9]							
1		5896	3+,5+				3+(t)	6	5965				
2		5959	3+,5+	*			5+(t)	7	6044				
3		5978	(9+)				9+(g)	3	5829				
4	8	6139	(7+)	(b)	(3,7)+	9	3+(t)	7	6141				
5	29	6160	(5−,7+)	(b)	7[+]	5				5−(t)	2	5825	
6	124	6255	1+	1+		1+	1+(g)	5	6259				$p1$
7	149	6280	3+	3+		3+	3+(g)	8	6280				$p2$
8	196	6327	(3)	(b)	3[−]	1+				3−(t)	2	6327	
9	226	6357	(5−)	(b)	5[−]	3+							
10	246	6377	(9−)	(9)	(5,9) [9−]	9[−]				9−(g)	1	6313	$n2$
11	261	6392	(5+)	(a),(5+)	5+		5+(g)	8	6402				$p3$
12	263	6394	(11+)	(a),(11)	11[+]	[11+]	11+(g)	1	6364				
13	270	6401		(a,c)			7+(t)	6	6298				
14	289	6421	(1+,3+,5+)	*									
15	411	6542	(3−)	(b)	3[−]	(7,9)				3−(t)	3	6757	$n3$
16	451	6583	(7)	(7)	(3,5,7)[−]	7				5−(t)	3	6792	
17	505	6636	(9−)	(9)	(5,9)[9−]	9[−]				9−(g)	2	6682	
18	589	6720	(5)			5	5+(t)	9	6862				$p4$
19	618	6749	3+			3+	3+(t)	9	6965				$p5$
20	665	6796		*									
21	702	6833	(11−)			11[−]				11−(g)	1	6833	
22	705	6836		*									
23	717	6848		*									
24	741	6872	(11)			11							
25	806	6937	(1+,3+,5+)			[(1-5)+]							
26	830	6961				[1+]	1+(t)	6	6995				
27	844	6975	1+				1+(t)	7	7028				
28	116									1−	2	6247	$n1$
29	471									1−	3	6602	$n4$

at 6796 keV has only been seen in a low resolution (^{3}He,n) experiment and has not been confirmed. The placement of two nearby levels at 6833 and 6836 keV was inferred from the fact that a significant proton emission was observed at this energy that may not be expected for a level with $J = 11/2^-$, which would decay by $\ell = 5$ [28]. Wrede has suggested that increased communication between the relevant experiment groups would facilitate some resolution of these experimental ambiguities [28].

Columns 11–13 give the results obtained with the $1\hbar\omega$ Hamiltonian. The k in column 12 is the number of the state for a given J. Columns 14 and 15 give the calculated spectroscopic factors. The labels in the last column indicate the contributions for the positive-parity p and negative-parity n rates as shown by the labels in Fig. 1.

Columns 8–10 give the results obtained with the USDB-cdpn Hamiltonian. The k in column 9 is the number of the state for a given J. All of the USDB-cdpn energies given have been shifted down by 240 keV in order to align theory and experiment for the well-established $3/2^+$ $T = 3/2$ level at 6280 keV. This gives energies for other positive-parity states in the region of interest within 100 keV of possible associations with experiment as shown in Table I. This shift was also noted in a recent experimental paper for γ decay of states in ^{31}S (see Fig. 7 in [24]). A similar energy shift is also found for the comparison of theory and experimental levels in ^{31}P, and it is also about the same with the USDA Hamiltonian. This shift indicates a possible systematic failure of the USD Hamiltonians at high energy. For future work it may be interesting to include some of these levels in the determination of the empirical two-body matrix elements [30]. Since the reaction rate is exponentially sensitive to the resonance energy, the association with the more precise experimental energies is important. Some of the associations in Table I are rather certain (good, g) but others are very tentative (t). All matches need to be confirmed. (There are two unmatched theoretical levels between 6.8 and 7.0 MeV not listed in Table I.)

With respect to the $1\hbar\omega$ calculations, the lowest $7/2^-$ and $3/2^-$ states in ^{29}Si and ^{29}P are dominated by $f_{7/2}$ and $p_{3/2}$ configurations, respectively, outside of the even-even ^{28}Si core. The energies of these four states were used to set the proton and neutron single-particle energies for these two orbitals and

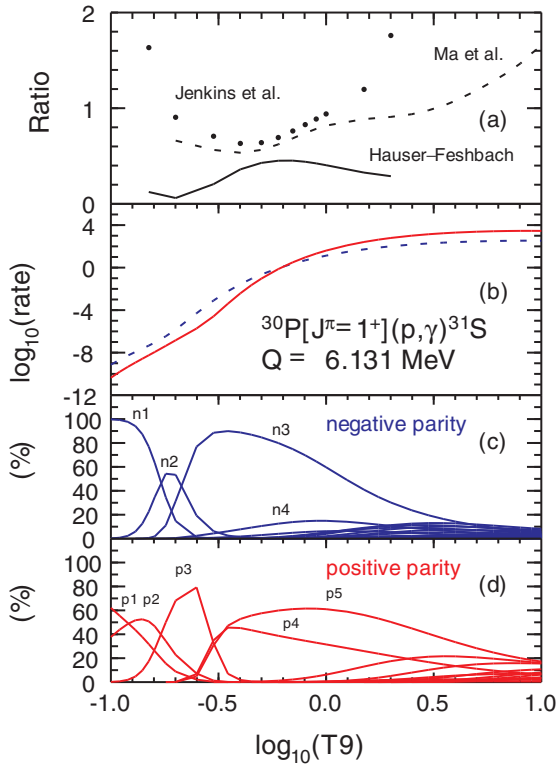

FIG. 1. (Color online) Panel (b) shows the ^{30}P ground state rp-process reaction rates $N_A\langle\sigma\nu\rangle$ (cm^2 s^{-1} mol^{-1}) versus temperature T_9 (gigaK) for the negative parity (blue dashed line) and positive parity (red line) final states. The relative contributions for each of the resonances is shown for negative-parity states in panel (c), and positive-parity states in panel (d). The top panel (a) shows the present rate divided by those from other models as discussed in the text.

typical spin-orbit splitting was assumed for the higher $f_{5/2}$ and $p_{1/2}$ orbitals. This adjustment takes into account the rather large Thomas-Ehrman shift for $3/2^-$, where the $3/2^-$ in ^{29}P is lowered by 600 keV compared to ^{29}Si. The proton and neutron excitations and related Thomas-Ehrman shifts in ^{31}S and ^{31}P are more complex since these have an odd-odd core. The energy of the $1/2^-$ state in ^{27}Si was used to fix the single-particle energy for $p_{1/2}$ with the $p_{3/2}$ energy placed lower at a typical spin-orbit splitting energy difference.

The energies for the $1\hbar\omega$ states in Table I are shifted down by 354 keV in order to align theory and experiment for the well-established $11/2^-$ level at 6833 keV. The theoretical levels have been associated with known experimental levels in Table I with the labels good (g) and tentative (t). This association is crucial for accurate calculations of the rates. Thus, the rates we obtain will depend upon a confirmation of the experimental and theoretical associations. The $1\hbar\omega$ states of possible importance for the rate that cannot be matched with experiment are given at the bottom of Table I (five other negative-parity states between 6.8 and 7.0 MeV that are not important for the rate are not listed). Lower lying negative parities that are not in Table I are predicted at (in units of MeV), 4.315 ($7/2^-$), 4.590 ($3/2^-$), 5.264 ($5/2^-$), 5.702 ($1/2^-$), and 6.056 ($7/2^-$). The only experimental state with a definitive spin-parity assignment is the $7/2^-$ state at 4.451 MeV.

All levels up to 6.8 MeV can be tentatively matched with theory except for the experimental levels at 6160, 6420, and 6796 keV; but the latter two of these are of questionable experimental existence. There are two $1/2^-$ states predicted at 6247 and 6602 that cannot be matched to known experimental levels. Above 6.8 MeV the two $1/2^+$ levels at 6961 and 6975 MeV have a good association with theory with the upper of these in theory being a candidate for the $1/2^+$ $T = 3/2$ level. In addition, between 6.8 and 7.0 MeV there are four unmatched experiment levels and seven theoretical levels, indicating that there are several levels in this region that have not yet been observed. The experimental information on states in the mirror nucleus ^{31}P in the 6–8 MeV energy range is not complete enough to help resolve the spin-parity ambiguities in ^{31}S or to help with the associations between experiment and theory we have made in Table I.

Our calculated rates are shown in Fig. 1 based on the resonance energies in Table I. They are based on the standard Eqs. used in [23] with the information in Table I together with γ-decay lifetimes for positive-parity states obtained with the USDB-cdpn Hamiltonian and the effective gamma-decay operator for $M1$ and $E2$ from [31]. The calculated $B(E1)$ for states below 7 MeV are small due to a cancellation between the single-particle components for low-lying configurations and those for the collective giant-dipole resonance (around 20 MeV) that contains the majority of the $E1$ strength. The reliability of these weak $E1$ should be checked by comparison with known $B(E1)$ between low-lying states. For the present rates we use a constant γ width of 9.1 meV corresponding to the average experimental half-life of about 50 fs for negative-parity states at this excitation in ^{31}P. The bottom parts of the figure show the contributions from individual final states. The labels for the most important contributions in Fig. 1 are those indicated on the right-hand side of Table I. For the hottest ONe novae on white dwarfs close to the Chandrasekhar limit the rate up to about $\log_{10}(T_9) = -0.3$ is important [32]. In this region our states $n1$-$n4$ and $p1$-$p5$ are most important. The numerical values for the total rates for negative- and positive-parity states are given in Table II. The calculated spectroscopic factors and widths for these states (in units of eV) are given in Table III. In the region of $\log_{10}(T_9)$ up to -0.3 the rate from negative-parity states is an order of magnitude larger than those for positive parity.

Figure 1(a) shows the present rate divided by those given by the Hauser-Feshbach (HF) model (solid line) [33], and the resonance state results based on the assumptions made by Jenkins *et al.* (filled circles) [11] and Ma *et al.* (dashed line) [14]. The rates for these are given in the Reaclib data base [34]. These previous rates are based on assumptions that are much less microscopic than the present. The HF results are 2–5 times larger than ours.

However, the reaction rates are much less certain than what might be implied from the ratios in Fig. 1(a). Several of the state associations between theory and experiment need to be verified. Theoretical uncertainties in the rates for the positive-parity states can be assessed by comparison of the results with the USDB Hamiltonian to those of USDA and USD [30]. The

TABLE II. Values for the ^{30}P ground state rp-process reaction rates $N_A\langle\sigma v\rangle$ (cm^2 s^{-1} mol^{-1}) versus temperature T_9 (gigaK) plotted in Fig. 1(b).

$\mathrm{Log}_{10}(T_9)$	Log_{10}(rate)	
	Negative parity	Positive parity
−1.000	−9.14	−10.4
−0.959	−8.66	−9.80
−0.921	−8.27	−9.33
−0.886	−7.93	−8.93
−0.854	−7.62	−8.57
−0.824	−7.34	−8.25
−0.796	−7.05	−7.94
−0.745	−6.46	−7.36
−0.699	−5.83	−6.83
−0.602	−4.30	−5.73
−0.523	−3.10	−4.59
−0.456	−2.22	−3.39
−0.398	−1.56	−2.41
−0.347	−1.05	−1.64
−0.301	−0.64	−1.04
−0.222	−0.05	−0.13
−0.155	0.37	0.50
−0.097	0.69	0.96
−0.046	0.93	1.32
0.000	1.11	1.60
0.097	1.48	2.10
0.243	1.88	2.63
0.398	2.17	3.01
0.544	2.35	3.23
0.699	2.47	3.38
1.000	2.53	3.46

major difference between USDA and USDB comes from the properties of the $5/2^+$ $(k = 8, p3)$ state due to a change of the $\ell = 2$ spectroscopic factor from 3.2×10^{-3} for USDB to 6.0×10^{-3} for USDA, resulting in a factor of 2 increase in the rate for USDA compared to USDB near $\log_{10}(T_9) = -0.6$.

The major difference with USD comes from the fact that the $3/2^+(k = 7)$, $T = 1/2$ state that is 139 keV lower than the $3/2^+(k = 8)$, $T = 3/2$ state with USDB (see Table I) becomes nearly degenerate with the $T = 3/2$ state, with USD resulting in a strong isospin mixing. This $T = 1/2$ state has a spectroscopic factor that is an order of magnitude higher than that of the $T = 3/2$ state. The rate for state $p2$ in Fig. 1 becomes an order of magnitude larger for USD compared to USDB. However, in the β decay of ^{31}Cl, only one strong γ decay is observed near 6280 keV (see Fig. 5.13 in [6]) indicating that there is no strong isospin mixing with a nearby $T = 1/2$ level. It is important to confirm our tentative assignment of the $3/2^+$, $T = 1/2$, $k = 7$ level with the experimental state at 6139 keV from the β decay of ^{31}Cl.

Theoretical uncertainties for the more important negative-parity states are much larger. In particular, the experimental positions of the $1/2^-$ states in Table I are not known. For example, if the state $n1$ were 200 keV higher than that given in Table I the rate around $\log_{10}(T_9) = -0.6$ would be an order of magnitude higher. The energy association for the 6542 keV $3/2^-$ $(n3)$ state needs to be verified and its γ width needs to be measured.

In summary, in view of the importance of the ^{30}P$(p,\gamma)^{31}$S reaction, we considered the major aspects leading to uncertainties in calculating the reaction rate. Because of the high excitation energies involved in the resonance region, several negative-parity states appear. Calculations were done for the first time in this mass region in a full $1\hbar\omega$ model space to take their contributions into account. In the region of astrophysical interest we predict that the negative-parity states are most important. The $1/2^-$ states have not yet been observed experimentally. This makes the rate uncertain by about an order of magnitude. Our calculations and results will guide the next generation of experiments.

This work is partly supported by NSF Grants No. PHY-1068217 and No. 1102511, the Joint Institute for Nuclear Astrophysics NSF Grant No. PHY08-22648, and the National Research Foundation of South Africa Grant No. 76898.

TABLE III. Properties of the most important theoretical levels for the ^{30}P$(p,\gamma)^{31}$S rate in the region up to $\log_{10}(T_9) = -0.3$. The γ widths given in parentheses are estimated from the average γ-decay widths for negative-parity states in ^{31}P.

n		Experiment [5]		Theory			Theory							
							USDB-cdpn			$1\hbar\omega$				
	E_{res} (keV)	E_x (keV)	$(2J)\pi$	Γ_γ (eV)	Γ_p (eV)	$\omega\gamma$ (eV)	$(2J)\pi$	k	E_x (keV)	$(2J)\pi$	k	E_x (keV)	ℓ	C^{2}S	
6	124	6255	1+	0.22	2.8×10^{-11}	9.5×10^{-12}	1+(g)	5	6259				0	1.7×10^{-3}	$p1$
7	149	6280	3+	0.97	1.6×10^{-10}	1.1×10^{-10}	3+(g)	8	6280				0	2.4×10^{-4}	$p2$
10	246	6377	(9−)	(0.009)	4.1×10^{-7}	6.9×10^{-7}				9−(g)	1	6313	3	0.39	$n2$
11	261	6392	(5+)	0.061	2.1×10^{-7}	2.1×10^{-7}	5+(g)	8	6402				2	3.2×10^{-3}	$p3$
15	411	6542	(3−)	(0.009)	0.19	5.8×10^{-3}				3−(t)	3	6757	1	0.029	$n3$
18	589	6720	(5)	0.40	0.088	0.072	5+(t)	9	6862				2	0.081	$p4$
19	618	6749	3+	0.63	0.56	0.20	3+(t)	9	6965				0	4.5×10^{-3}	$p5$
28	116			(0.009)	3.0×10^{-10}	1.0×10^{-10}				1−	2	6247	1	0.23	$n1$
29	471			(0.009)	0.19	2.9×10^{-3}				1−	3	6602	1	0.068	$n4$

[1] S. Amari, X. Gao, L. R. Nittler, E. Zinner, J. Jose, M. Hernanz, and R. S. Lewis, Astrophys. J. **551**, 1065 (2001).
[2] C. Iliadis, A. Champagne, J. Jose, S. Starrfield, and P. Tupper, Astrophys. J. Suppl. Ser. **142**, 105 (2002).
[3] J. Jose, M. Hernanz, S. Amari, K. Lodders, and E. Zinner, Astrophys. J. **612**, 414 (2004).
[4] K. J. Kelly, C. Iliadis, L. Downen, J. Jose, and A. Champagne, Astrophys. J. **777**, 130 (2013).
[5] C. Ouellet and B. Singh, Nucl. Data Sheets **114**, 209 (2013).
[6] A. Saastamoinen, Ph.D. thesis, University of Jyvaskyla, 2011.
[7] D. Irvine *et al.*, Phys. Rev. C **88**, 055803 (2013).
[8] D. T. Doherty *et al.*, Phys. Rev. Lett. **108**, 262502 (2012).
[9] A. Parikh *et al.*, Phys. Rev. C **83**, 045806 (2011).
[10] D. G. Jenkins *et al.*, Phys. Rev. C **72**, 031303 (2005).
[11] D. G. Jenkins *et al.*, Phys. Rev. C **73**, 065802 (2006).
[12] C. Wrede, J. A. Caggiano, J. A. Clark, C. M. Deibel, A. Parikh, and P. D. Parker, Phys. Rev. C **76**, 052802 (2007).
[13] H. Nann and B. H. Wildenthal, Phys. Rev. C **19**, 2146 (1979).
[14] Z. Ma *et al.*, Phys. Rev. C **76**, 015803 (2007); **76**, 039901(E) (2007).
[15] C. Wrede, J. A. Caggiano, J. A. Clark, C. M. Deibel, A. Parikh, and P. D. Parker, Phys. Rev. C **79**, 045803 (2009).
[16] J. Vernotte *et al.*, Nucl. Phys. A **655**, 415 (1999).
[17] P. M. Endt, Nucl. Phys. A **521**, 1 (1990).
[18] P. M. Endt and C. Van der Leun, Nucl. Phys. A **310**, 1 (1978).
[19] P. M. Endt, J. Blachot, R. B. Firestone, and J. Zipkin, Nucl. Phys. A **633**, 1 (1998).
[20] L. N. Downen, C. Iliadis, J. Jose, and S. Starrfield, Astrophys. J. **762**, 105 (2013).
[21] W. A. Richter, B. A. Brown, A. Signoracci, and M. Wiescher, Phys. Rev. C **83**, 065803 (2011); **84**, 059802 (2011).
[22] W. A. Richter and B. A. Brown, Phys. Rev. C **85**, 045806 (2012).
[23] W. A. Richter and B. A. Brown, Phys. Rev. C **87**, 065803 (2013).
[24] D. T. Doherty *et al.*, Phys. Rev. C **89**, 045804 (2014).
[25] NuShellX@MSU, B. A. Brown, W. D. M. Rae, E. McDonald, and M. Horoi, www.nscl.msu.edu/~brown/resources/resources.html
[26] E. K. Warburton and B. A. Brown, Phys. Rev. C **46**, 923 (1992).
[27] E. K. Warburton, J. A. Becker, and B. A. Brown, Phys. Rev. C **41**, 1147 (1990).
[28] C. Wrede, AIP Advances **4**, 041004 (2014).
[29] A. Kankainen *et al.*, Eur. Phys. J. A **27**, 67 (2006).
[30] B. A. Brown and W. A. Richter, Phys. Rev. C **74**, 034315 (2006).
[31] W. A. Richter, S. Mkhize, and B. A. Brown, Phys. Rev. C **78**, 064302 (2008).
[32] S. A. Glasner and J. W. Truran, Astrophys. J. **692**, L58 (2009).
[33] T. Rauscher and F. K. Thielemann, At. Data Nucl. Data Tables **75**, 1 (2000).
[34] The JINA Reaclib Database, H. Cyburt *et al.*, Astrophys. J. Suppl. **189**, 240 (2010).